

The Separation of Beaded Chains in a Two Dimensional Confined Environment

by

Justin Bondy

A thesis submitted in conformity with the requirements
for the degree of Master of Science
Graduate Department of Physics
University of Toronto

Copyright © 2012 by Justin Bondy

Abstract

The goal of this project was to study two dimensional entropically driven separation of two long beaded chains. This was accomplished by placing two brass chains initially mixed in a long 2D slot and observing their behavior as the slot is shaken. The motivation for this was to create an experimental analog for the separation of chromosomes during bacterial cell division. The two main factors that were tested to see how they affect chain separation were the confinement of the chains and the asymmetry of the container they were held in. It was predicted from theory and past simulations that increasing chain confinement and container asymmetry would increase the strength of the chain separation. Three methods of analysis were performed on the experimental data. A method that measured the length of the region that the two chains were overlapping each other, as well as dividing the container into 2D and 1D grids and counting the density of beads in each bin. An surprising result was the formation of tight spiral conformations, which were not expected to be formed in the frequency/acceleration regime we were testing in. These spirals occurred in $\sim 40\%$ of all chain configurations observed and polluted the data as their ratcheting motion was not the entropically driven forces we wished to study. No discernible trends were observed with regards to the effect of confinement or container geometry on chain separation.

Acknowledgements

First and foremost I would like to thank my supervisor Stephen Morris. His confidence in the project and my abilities, as well as his enthusiasm for science, were a great inspiration to me during this projects duration. I am most thankful for his practicality. Whenever I would become overwhelmed at the potential scope this project could encompass he would always calm me down and remind me to take things one step at a time.

I would also like to thank Will Ryu, whose drive and ambition were a constant source of motivation for me to strive for excellence. Whenever we would meet I would come away with a plethora of new ideas and angles on how to tackle problems I was encountering. I would also like to thank my friends and colleagues, particularly Antony Chen. Though we worked on different floors, it was always a boon to have another student to discuss ideas and frustrations with.

Lastly I would like to thank my family. I can truly say that I would not have been able to accomplish what I have without my parent's emotional (and occasionally financial) support. Whenever I would start to flounder at some difficulty, whether academic or personal, knowing I had the unwavering support of my parents would always be a great help. My sister's amazing confidence in her little brother was greatly appreciated, and is always humbling.

Contents

1	Introduction	1
1.1	Motivation	1
1.2	Literature Review	2
1.3	Entropy of Mixing	2
1.3.1	Free Energy of Mixing	3
1.4	Effect of Container Symmetry on Segregation	4
2	Experiment	5
2.1	Apparatus	5
2.2	Run Preparation	7
3	Analysis	11
3.1	Image Analysis	11
3.2	Data Analysis	13
3.2.1	Overlap Method	13
3.2.2	2-Dimensional Binning	14
3.2.3	1-Dimensional Binning	17
3.3	Spirals	18
4	Results and Discussion	21
4.1	Spirals	22
4.2	Effects of Confinement	25
4.2.1	Overlap Method	25

4.2.2	2-Dimensional Binning	27
4.2.3	1-Dimensional Binning	29
4.3	Effects of Container Symmetry	31
4.3.1	Overlap Method	32
4.3.2	2-Dimensional Binning	32
4.3.3	1-Dimensional Binning	35
4.4	Discussion	35
4.4.1	Future Work	37
4.5	Conclusion	37
	Bibliography	38

List of Figures

2.1	Apparatus: Shaking Plate	6
2.2	Apparatus: Camera	7
2.3	Schematic of the complete apparatus.	8
2.4	Sample Chain	8
2.5	Determining the radius of gyration.	9
2.6	Typical starting conditions for an experimental run.	10
3.1	Determining bead location	12
3.2	Determining overlap region	14
3.3	Example chain overlap.	14
3.4	Example of 2D binning on a mixed state.	16
3.5	Example of 2D binning on a relatively unmixed state.	16
3.6	Example of 1D binning on a mixed state.	17
3.7	Example of 1D binning on a relatively unmixed state.	18
3.8	Example of a tight spiral forming	19
3.9	Classifying spirals	20
4.1	Spirals as a function of confinement	23
4.2	Spirals as a function of symmetry	23
4.3	Spiral time series	24
4.4	Separation vs confinement: overlap method	26
4.5	Separation vs confinement: overlap method (spirals removed)	26
4.6	Overlap time series	27

4.7	Chain encircling another	27
4.8	Separation vs confinement: 2D binning method	28
4.9	Separation vs confinement: 2D binning method (Spirals removed)	28
4.10	Chains tightly wound around each other	29
4.11	2D binning time series	29
4.12	Separation vs confinement: 1D binning method	30
4.13	Separation vs confinement: 1D binning method (Spirals removed)	30
4.14	1D binning time series	31
4.15	Phase space measured over	32
4.16	Separation vs symmetry: overlap method	33
4.17	Separation vs symmetry: overlap method (Spirals removed)	33
4.18	Separation vs symmetry: 2D binning method	34
4.19	Separation vs symmetry: 2D binning method (Spirals removed)	34
4.20	Separation vs symmetry: 1D binning method	36
4.21	Separation vs symmetry: 1D binning method (Spirals removed)	36

List of Tables

4.1	Chains used to measure effects of confinement	21
4.2	Chains used to measure effects of symmetry (low confinement)	22
4.3	Chains used to measure effects of symmetry (high confinement)	22

Chapter 1

Introduction

The experiment discussed in this report primarily concerns the two dimensional separation of two long beaded chains initially mixed in a confining container as they are driven on a shaking table. The primary focus was to treat these chains as an analog for chromosome separation in bacterial cells, though the scope widened to include investigation into less biologically motivated measures of granular chain separation.

1.1 Motivation

The original motivation for this report was to provide experimental confirmation for simulations regarding the separation of long polymer chains under confined conditions. These simulations were themselves motivated by the idea of explaining the separation of bacterial chromosomes during cell division, with entropy proposed as the primary driver of separation.

Cell replication is the fundamental process from which all life continues to grow and expand. One of the most important processes that occur during cell division is the replication and segregation of chromosomes; the organized structure that houses the cells genetic instructions of the cell. Understanding how chromosomes are copied and organized during the cell cycle is of critical importance, as many harmful genetic mutations may occur if this process contains errors, whether they be caused by random chance or harmful outside forces. This process is well understood in eukaryotic cells, but the method by which this is accomplished is still under investigation for prokaryotes (such as bacteria like E. Coli).

1.2 Literature Review

In Eukaryotic cells (complex cells with a nucleus and other membrane bound organelles) the process of chromosome separation is well understood. In these cells the chromosomes are packed into nucleosomes around positively charged histone proteins, and after their replication they are pulled to the poles of the cell by a dedicated cytoskeletal apparatus [1]. However these tools of eukaryotic cell division do not appear in simpler prokaryotic cells. In fact, the mechanism behind the segregation of the replicated chromosomes in prokaryotes is still a mysterious and highly debated topic.

Several theories have been put forward in the past to explain how bacterial chromosome separation is accomplished. Some of these ideas include chromosomes being pulled apart by the expanding cell wall [2], or the chromosomes being exuded to the sides during their creation by a replisome held stationary in the cells center [3], while a similar idea claimed the chromosomes were repelled by RNA polymerase in the cell center [4]. However, all these ideas were eventually disproved for various reasons (see [5], [6], and [7] respectively).

In 2006 Jun and Mulder presented a model that used entropic forces as a means to drive spontaneous segregation [8]. In this model the chromosomes are considered to be polymer chains that drift apart towards the less crowded space near the cell walls to maximize their conformational entropy and minimize the free energy contained in the system.

1.3 Entropy of Mixing

An excellent review of entropic effects in systems of mixing particles compared to mixing chains is presented by Jun and Write [9]. The classic example of maximizing the entropy of a system is that of a box containing two different species of particles initially separated by a barrier. As the barrier is removed the particles readily mix, as this is the result with the highest entropy due to there being many more mixed configurations than unmixed configurations. In contrast, we can investigate the case of a box with two long linear chains initially mixed together. Unlike the particle case, entropic forces instead cause these two chains to become unmixed. To understand this result imagine placing a string on a flat surface in a tightly confined box and then attempt to place another string in the same box

without the chains crossing. It is much more difficult to find overlapping (but not crossing) configurations, than it is if both chains simply occupy one corner of the box instead of being mixed. In other words overlapping chains have less degrees of freedom, and thus less conformational entropy than separated chains. Similar to the particle example, the chains are more likely to end up in the state that offers the most possible configurations (that being the unmixed state).

1.3.1 Free Energy of Mixing

We can get an idea of the kinds of factors that affect separation by investigating the free energy of a mixed system. Flory and Krigbaum [10] originally presented the idea that the free energy of overlapping two chains scales as $F \sim N^{1/5}k_B T \gg k_B T$, where N is the number of monomers in each chain and k_B is Boltzmanns constant. This expression indicates that long chains ($N \gg 1$) should behave as mutually impenetrable hard spheres that strongly resist mixing. However, Grosberg et al. [11] eventually reevaluated this result and instead came up with the expression for the free energy cost as $F \sim k_B T$, where we can see the cost is both independent of chain length and rather weak, suggesting that chromosomes should have no strong preference to unmix. Both of these expressions, however, are for the case of long polymer chains in a dilute solution with no confinement, which is not applicable to a model of bacterial geometry (which is highly confined), or this experiment.

The more relevant scenario to bacterial cells is chains confined in a long cylinder (3D) or slot (2D) with a high level of confinement. Confinement is measured by the ratio of the radius of gyration of the polymer over the diameter of the container (R_g/D). R_g is the radius of the area the polymer would naturally occupy if it was not confined. In this case the free energy cost of mixing is $F \sim D^{-1/v} N k_B T$ where $v \cong 3/5$ [8]. As we can see, this result has a strong dependence on both the length of the chains and on how confined they are. Therefore long chains in very strong confinement have the highest free energy cost for overlapping and thus most readily segregate from each other. It should also be noted that cyclical chromosomes, like those present in bacteria, segregate more readily than linear polymers [12]. It is, however, much easier to perform experiments with linear rather than

looped chains, and if linear chains are found to separate it should follow that loops will as well, as the separation effect is greater.

1.4 Effect of Container Symmetry on Segregation

Once we know that confinement should have a strong effect on how the polymers separate, we can investigate how the container shape could also effect it. In particular Jacobsen [13] purports that container asymmetry plays an important role in long chain separation. He studied computer simulations of two self-avoiding chains in three-dimensionally lattices with the shape $L \times L \times rL$, where r is the scaling factor (high r gives high asymmetry, $r = 1$ is perfectly symmetric). The simulation consisted of two long chains whose monomers occupied nearly every lattice site at all times, and a Monte Carlo simulation was performed to determine the statistical likelihood of different configurations occurring. It was found that separation of the chains did occur with all lattice shapes, though very weakly in the symmetric case. The more asymmetric the container became the stronger the separation became (though perfect separation did not occur, even at the limit of $r = 10$). This led us to experimentally study how changing the shaking tables slot diameter, but not its length (thus changing the slots symmetry) affects the chain separation.

Chapter 2

Experiment

The experiment involves shaking initially mixed beaded chains in a two dimensional slot as a scaled up, physical analog for the separation of chromosomes in bacteria during cell division. As discussed in the introduction the current theory on how chromosomes separate is based on entropy, so this experiment focuses on how entropy may drive separation of two chains in a two dimensional slot with a shaking table taking the place of random thermal motion in bacterial cells. We shake two initially mixed chains for long times over a range of parameters, and observing how these parameters affect the separation of these chains. The chains used are common brass beaded chain (commonly used for things like light bulb pull switches) purchased from McMaster-Carr. Originally multiple bead sizes were planned to be tested, but due to time constraints only chain with 0.237cm bead diameter were tested.

2.1 Apparatus

The primary piece of the apparatus is a 25.4cm x 25.4cm aluminum plate that has been anodized black to provide contrast for the beaded chain. This plate has four 3.2cm high walls that have been machined with long horizontal slots to allow the placement of adjustable internal walls. These internal walls can be moved around to obtain any slot size we desire (for example 7.6cm x 25.4cm). The plate and walls can be viewed in Figure 2.1.

The plate is driven by a Model ET-140 Electrodynamic Shaker powered by a Model PA-141 Power Amplifier purchased from Labworks Inc. The shaker has a 1" peak-to-peak

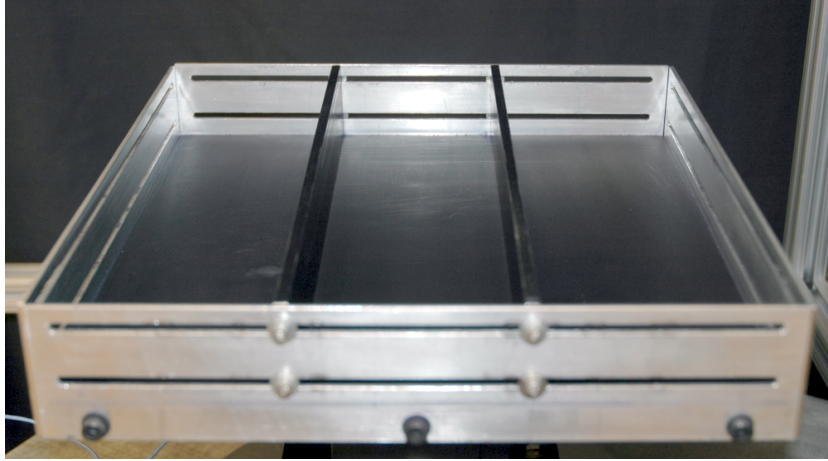


Figure 2.1: Anodized aluminum plate with adjustable internal walls.

maximum displacement, a maximum sine force output of 100 lbf, and a frequency range of DC to 6.5 kHz providing more than enough power and versatility for our needs. To control the amplitude and frequency of the shaker it is connected to a Agilent 33120A Waveform Generator. Measurements of the acceleration experienced by the plate and load were gathered using a PCB Piezotronics Model 356B08 Accelerometer connected to a computer with a National Instruments NI SCXI-1303 control module.

To analyze the chains as they are shaken a Canon Rebel T2i was attached to a metal frame $\sim 0.7\text{m}$ above the plate. Canon's commercial EOS camera control program is used to set the camera to take a picture every 5 seconds. Uniform illumination is provided by an array of white LEDs circled around the camera lens projecting downwards towards the plate. The camera and LED array is shown in Figure 2.2.

The chain used consisted of many hollow brass spheres attached with thin rods. The spherical beads were $0.237 \pm 0.001\text{cm}$ in diameter, while the rod diameter was $0.061 \pm 0.002\text{cm}$. The beads were permitted by the rods to move anywhere from 1 to 1.37 bead diameters apart (measured center to center). The smallest circle the beads are able to form consisted of 8 beads (giving a persistence length of 2.5cm), with the rods forming a 40° angle to each other.

A major obstacle that was encountered with the shaker system was small but noticeable horizontal movements of the shaking plate when driven in the vertical direction. This was



Figure 2.2: Canon Rebel T2i and LED array used to capture images of shaking chains.

caused by the weight of the load not being perfectly distributed across the plate which would caused the shaker to buck slightly to the side with more weight during its throw cycle. This forced even more material to move towards the uneven side of the plate creating a positive feedback loop that increases this undesired horizontal motion until all of the load has shifted to the uneven side. To prevent this from occurring we installed a linear air bearing purchased from New Way Air Bearings. The plate was attached to a peg which was machined to only fit through a vertical square slot when compressed air is supplied as a lubricant. The air bearing slot was attached to a heavy aluminum table to prevent movement, so the plate was unable to deviate from the vertical motion. To further increase the stabilizing effects of the air bearing, the plate/peg was connected to the driving shaker with a thin ($\sim 0.11\text{cm}$ diameter) piece of steel piano wire rather than a rigid piece of metal. This was done to prevent any horizontal motions of the shaker translating to the plate, as the piano wire could bend instead of translating this motion. A schematic of the complete apparatus is displayed in Figure 2.3

2.2 Run Preparation

As mentioned above, the chains we used are beaded brass chain with a bead diameter of 0.237cm (as seen in Figure 2.4). Originally we planned to use two different kinds of chain in the same experiment (brass and nickel) to make it easier to visually distinguish between the two chains used in a particular run. However, it was found that the properties of the

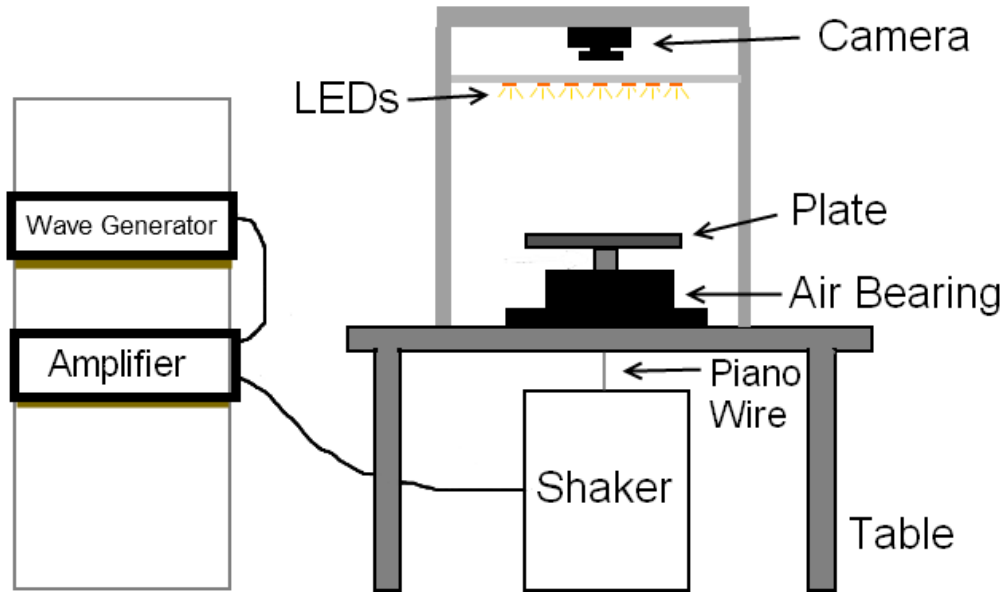


Figure 2.3: Schematic of the complete apparatus.

different chains were too dissimilar to be a good analog for the bacterial case where the separating chromosomes are identical. After experimenting with various alternatives we settled on using brass for both chains, but coloured one chain blue and the other red.



Figure 2.4: Simple brass beaded chain used.

When a particular length of chain is required for a run, two lengths of this chain (one to become red, the other blue for a single run) are cut to length. Each chain is then coloured using felt tip permanent markers twice to ensure an even coating. If shaken at this point the colouring very quickly rubs off due to the vigorous motion, so two layers of clear varathane are applied over the colouring. This allows the chains to last between one to two hours of shaking before enough colour is lost that they are no longer distinguishable. Using this method we ensure that the chains have the same statistical properties, namely radius of gyration (R_g) as seen in Figure 2.5. To determine R_g we cut several lengths of chain ranging from 5 to 23 cm and individually placed them on the open plate (no slot). We proceeded

to record them being shaken at the chosen frequency. We then analyzed these images to determine each chain lengths R_g according to the following formula :

$$R_g^2 = \frac{1}{2N^2} \sum_{n=1}^N \langle (R_n - R)^2 \rangle$$

Where N is the number of beads that comprise the chain, R_n is the location of the n^{th} bead and R is the location of the chain's center of mass [14]. R_g of a chain of arbitrary length can be extrapolated from this data using either of the following formulas:

$$R_g/d = 8.5 * N^{0.29} - 14.2$$

or

$$R_g = 2.6 * L^{0.3} - 3.1$$

where L is the length of the chain in cm and d is the diameter of the beads.

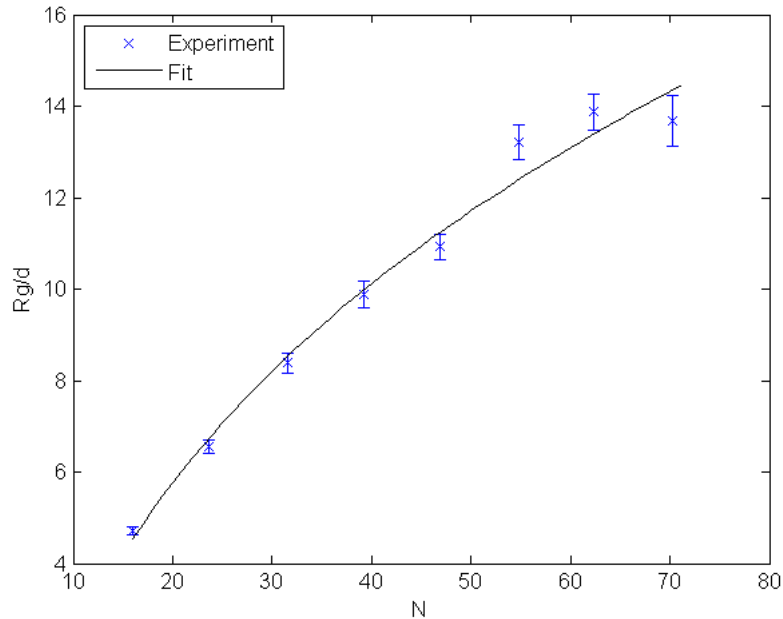


Figure 2.5: Determining the radius of gyration.

Once the chains is prepared they are placed into the slot size of our choosing in an

initially mixed state like the example shown in Figure 2.6. The appropriate shaking frequency and amplitude are selected and the shaking of the chains is recorded by the camera until the colour has worn off the chains. Initially our experiment operated at 60Hz, but for reasons discussed in a later section this was changed to 20Hz. When selecting the operating acceleration the plate and load would experience it was desirable to give as much energy as possible into the system so the chains could explore all possible configurations. However, since this was intended to be a two dimensional experiment, we did not want any chains crossing to occur during the shaking. Therefore this provided an upper limit to how much acceleration they could experience. It was found that an acceleration of 2.35 g's was the highest acceleration that did not have a significant amount of crossings occurring (random crossing did happen infrequently, but they also would often uncross themselves eventually).

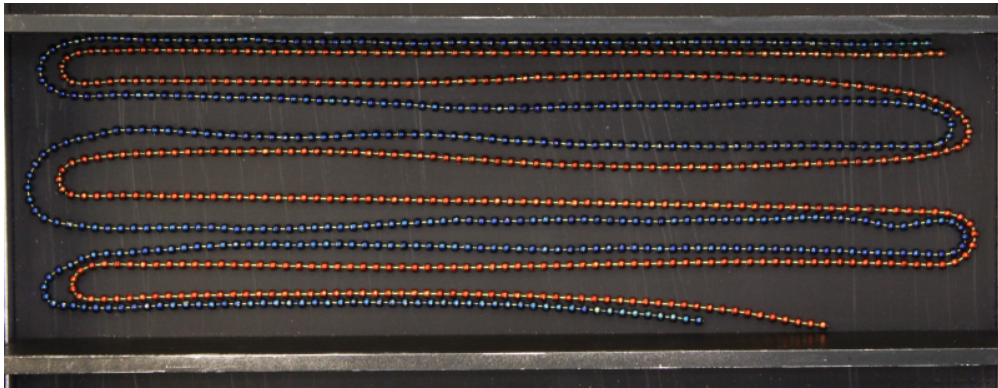


Figure 2.6: Typical starting conditions for an experimental run.

Chapter 3

Analysis

This chapter is primarily concerned with explaining how specific types of analysis were approached and accomplished, the results of which will be covered in the following chapter

3.1 Image Analysis

A typical run lasts between 1.5 to 2 hours, with around 1000 to 1500 pictures taken 5 seconds apart. These pictures are loaded into MATLAB for analysis, with the first step being finding the location of all the beads of each chain. This can be quite computationally expensive, especially as chains grow longer and contain more beads to locate. With long chains (ex. $N = 2000$) it can take up to 3 minutes to analyze a single picture. In the interest of time every 5th picture is analyzed in most runs, leading to 25 seconds of shaking time between each data point. Initially it is very easy to distinguish between the red and blue chains based on their colours, but as a run goes on these colours wear down significantly. Since the analysis is automated for large batches of pictures it is important to set conditions that will correctly identify which chain a particular bead comes from for the entire run. This is accomplished by noticing that though the colours of the beads fade, the ratios of the intensities of these colours does not change quite as rapidly. To find the location of the beads in the red chain we therefore subtract some of the blue channel from the red channel of the image data, then set an appropriate threshold that lets the red beads pass but background elements (or the blue beads) do not. It is then trivial to find the center of all the elements that survived the

thresholding. The same is done for the blue chain by subtracting some red channel from the blue channel of the image. This process is laid out in Figure 3.1.

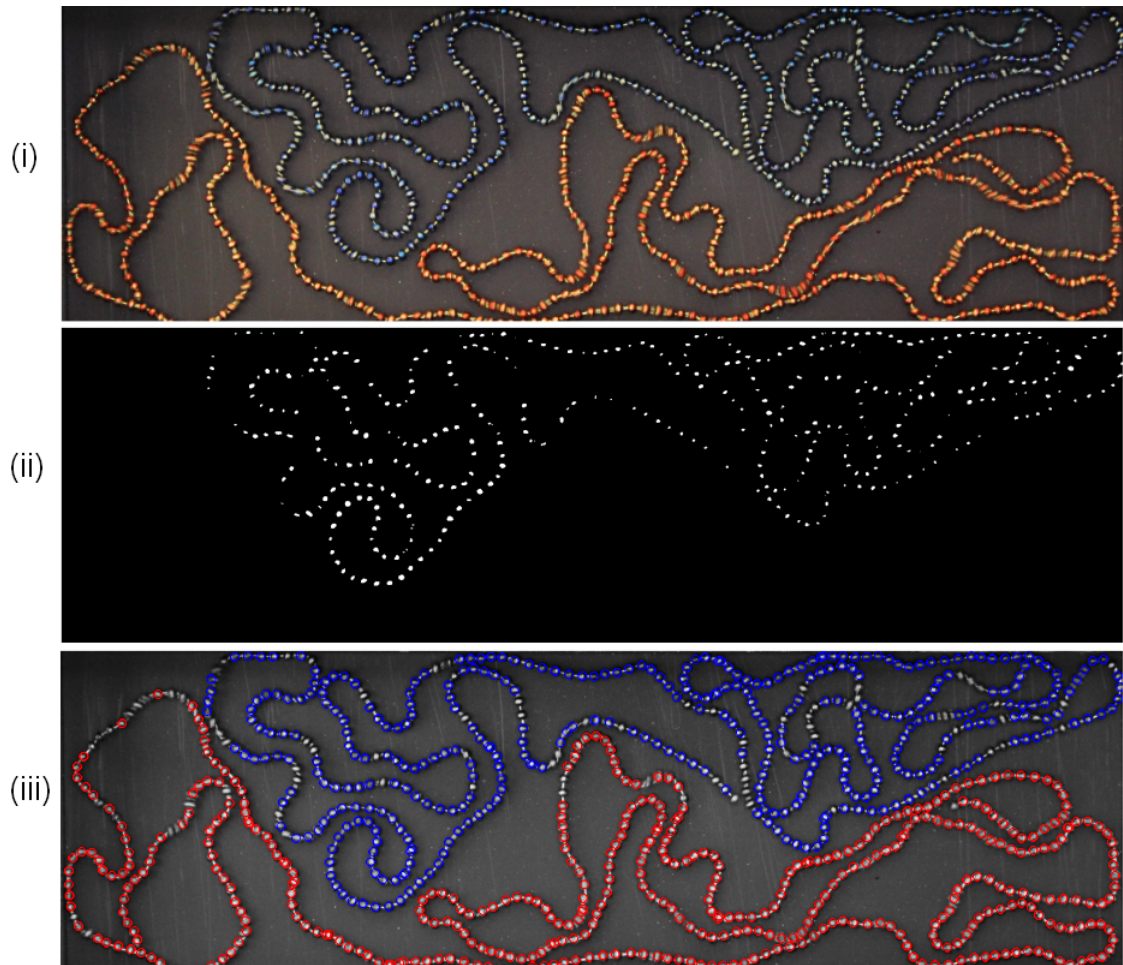


Figure 3.1: The process of locating the coloured beads on each chain. (i) Original Picture, (ii) Image thresholded to allow above a certain blue-red value (finding the blue beads), (iii) Predicted location of each colour bead overlaid on greyscale original image.

As is visible in Figure 3.1, not every bead is successfully located in all pictures. In order to ensure no beads of the wrong colour are counted as their opposite, the threshold value must be rather strict. This leads to some beads not being counted at all if their colour wears off too fast or in the wrong way. It is much better for some beads to not be counted than counting a bead as the wrong colour so this was considered acceptable. For an unknown reason the blue colour seemed to wear off faster, so the number of uncounted blue beads was generally higher than the uncounted red beads. As expected the number of uncounted

beads increases the longer the chains are shaken as they are worn down. On average, the percentage of beads that are correctly counted is as follows:

$$Counted_{Red} = 88 \pm 10\%$$

$$Counted_{Blue} = 79 \pm 11\%$$

3.2 Data Analysis

Once a picture is analyzed the location of each bead is stored for later analysis by one of the following methods to determine the extent of chain separation.

3.2.1 Overlap Method

This method is the closest analog to the biological case we originally set out to experimentally replicate, and was inspired by a recent 2012 paper by Jung et al. [15]. The main idea is to determine the fractional overlap distance of the two chains; meaning what percentage of their length is in an overlapping region with the other chain. As illustrated in Figure 3.2, the overlap region λ is measured along the length of the slot (hereby referred to as the z direction) where the two chains occupy the same z coordinates. More specifically λ is measured from the farthest blue bead in the region occupied by the red beads to the farthest red bead in the region occupied by the blue beads. Recall that this method is attempting to emulate the biological scenario of chromosome separation in cell division. Biologically it is important for the chromosomes to be separate at opposite ends of the cell, so even one monomer overlapping with the other chromosome would result in replication failure when the cell is cleaved in half at the end of the separation cycle. Thus this method is only concerned with how separated the chains are in the z -direction. The degree of mixing, which is the primary means we will use to discuss how the chains have separated, is the overlap region λ divided by the length L of z directional space occupied by the “shorter chain” (meaning the chain that occupies less space in the z -direction), λ/L .

The reason for defining L as the z -directional space occupied by the shorter of the two chains is show by an example in Figure 3.3. A natural thought would be to set L as the length of the region occupied by the chains in general (eg the farthest beads, regardless

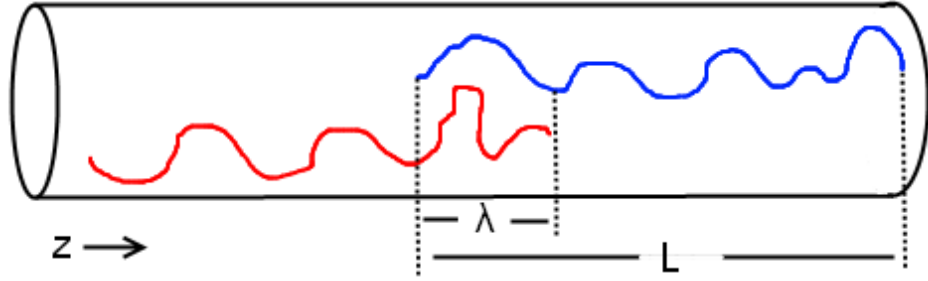


Figure 3.2: Illustrating how the overlap region λ and chain length scale L are determined.

of colour, at each end as the borders of L), but this would cause problems with how we interpret what is mixed or separated. In the example the overlap region is the entirety of the space occupied by the red chain as it is entirely overlapping in the z direction with the blue chain. If we choose L to be the entire region occupied by both chains we can see that $\lambda/L \cong 0.5$, when in reality it should be measured at completely mixed ($\lambda/L = 1$). Measuring L to be the area occupied by the chain taking up less space in z does in fact fix this problem and gives the correct degree of mixing of 1. This method is computationally rather simple as it only requires a program to locate the farthest beads of each type that occupy overlapping z coordinates.



Figure 3.3: Example chain overlap.

3.2.2 2-Dimensional Binning

We may not wish to only analyze the data taken with the biological case in mind, but instead study it purely as the separation of two linear granular chains. One possible method of determining the degree to which the chains have separated is to divide the slot into a 2

dimensional grid and count how many of each colour bead are in each box (or bin). This method has the property of measuring separation on the bases of how bunched together each chain becomes with itself at the exclusion of the other chain. Once we know how many of each bead are in each bin we multiply the number of red beads in the bin by the number of blue beads in the bin. The idea is that if the box is only filled with one bead type it would correspond to a completely separated bin; and multiplying the number of each type of bead in that bin would be some number multiplied by zero, which would in turn give that bin a mixing factor of 0. However, if there is at least one of each bead in a specific bin that bin is considered at least partially mixed, and the more of each bead type in the bin the more mixed it would be. Multiplying the number of beads together in this case would give a non-zero value that increases along with increases in the number of beads of each type in the bin, which matches our interpretation of the bin becoming more mixed. This value also favours equal numbers of each type of beads over a large number of one bead type with a small number of the other. For example, if there is 9 blue beads with 1 red bead the count would read a value of 9, but if there are 5 beads of each type the count would give a value of 25. This is desired as 5 of each type is much more mixed than 9 and 1, so it fits that it gives a higher value. An example of this method is given for a mixed and relatively unmixed configuration of beads in Figure 3.4 and 3.5 respectively. You can see that when the chains seem more mixed there are many more non-zero bins and the bins have higher values in general.

The actual measure of separation is found by taking the sum of each of these bins and normalizing them so completely unmixed is found to be 0 while uniformly mixed is found to be 1. This normalization is simply the number of bins measured over (referred to as B) divided by the products of the total number of red and blue beads in the entire picture. The degree of mixing is therefore calculated as:

$$\text{Degree of Mixing} = \frac{B}{N_{red}N_{blue}} \sum_{i=1} n_{red_i}n_{blue_i}$$

Where N is the total number of a particular colour of bead in the entire picture, and n_i is the amount of a particular colour of bead in the i^{th} bin. It should be noted that a

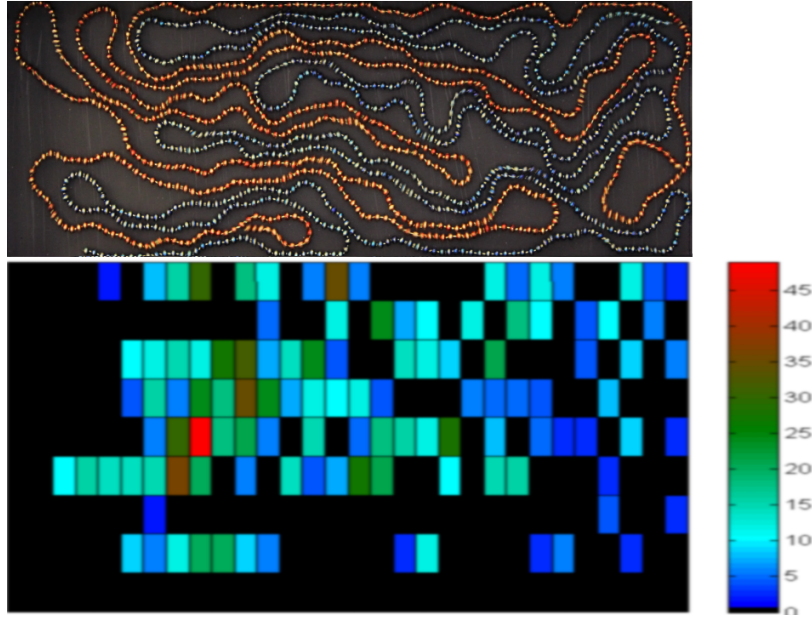


Figure 3.4: Example of 2D binning on a mixed state.

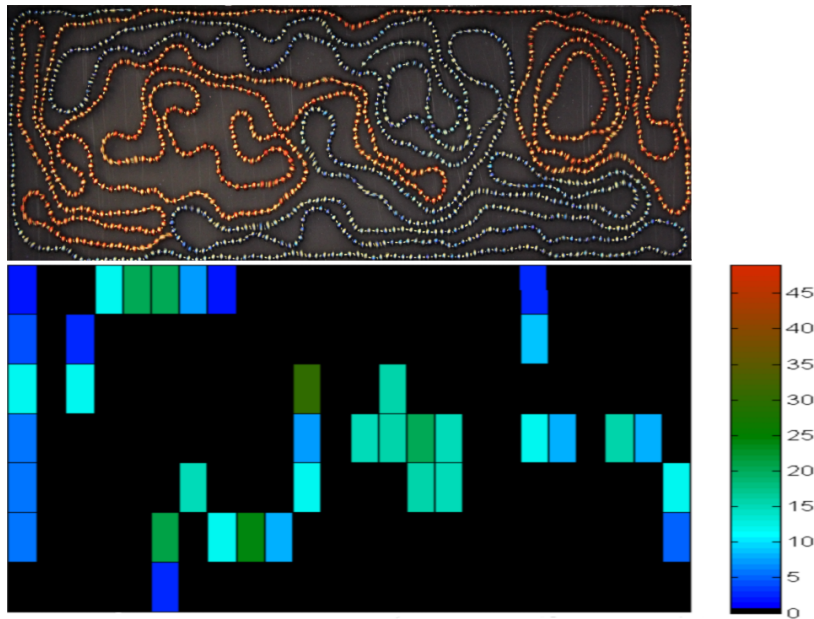


Figure 3.5: Example of 2D binning on a relatively unmixed state.

mixing value of 1 is given when the chains are perfectly mixed across the entire slot, but if they become entangled in each other very tightly and occupy only a small portion of the slot the mixing value from this formula can reach values greater than 1. While this is completely incompatible with the biological case, as a chain completely surrounded by

the other chain may be considered separated in this method, it still gives insight into the physics of separating chains in two dimensions.

3.2.3 1-Dimensional Binning

Similarly, we can divide the slot into a one dimensional grid in the z direction. This method is somewhere in-between the overlap and two-dimensional binning method. It is concerned with the separation of the chains along the length of the slot (like the overlap method and real biological case), but has the advantage that it also takes into account how much material is overlapping instead of just the size of the overlap region. While in the biological case even a small amount of overlap during cell division may cause serious genetic consequences, if we are just concerned with the separation of polymers or chains as a whole than a small amount of material overlapping should not be cause to claim the chains are completely mixed.

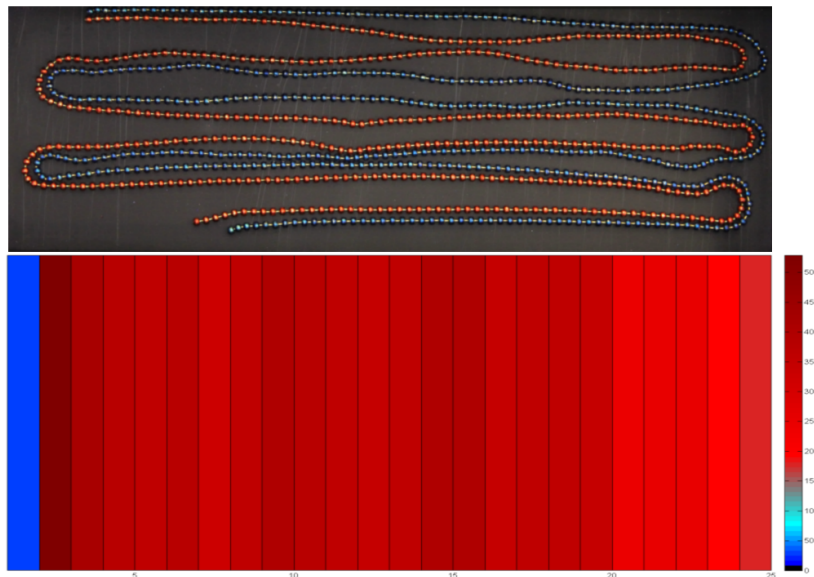


Figure 3.6: Example of 1D binning on a mixed state.

Just like the two-dimensional case, we divide the slot into bins and count the number of each colour bead in each bin. We multiply the number of beads in the bin together, sum over all the bins and normalize by the total number of beads in the box and the number of bins used. An example of a mixed and unmixed picture being analyzed in this way can

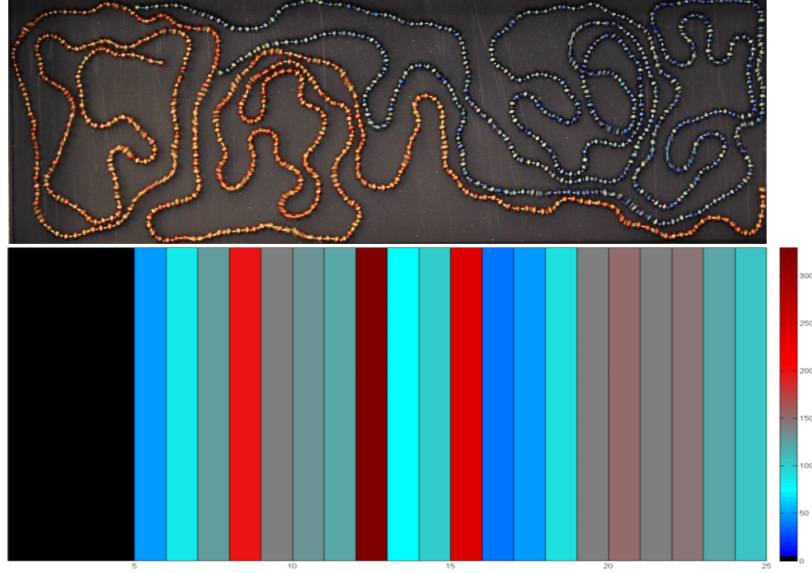


Figure 3.7: Example of 1D binning on a relatively unmixed state.

be seen in Figures 3.6 and 3.7 respectively. The degree of mixing is the same as for the 2-dimensional case, but summed along only one dimension :

$$\text{Degree of Mixing} = \frac{B}{N_{red}N_{blue}} \sum_{i=1} n_{red_i} n_{blue_i}$$

3.3 Spirals

A major unexpected obstacle we encountered was the formation of tight spirals formed by the chains, as shown in Figure 3.8.

The forming of these spirals has been documented before by Ecke et al [16], though it was a surprise they appeared in this experiment. In the experiment performed by Ecke et al. spirals were found to only form in a very tight range of parameters, these being dimensionless accelerations ($\Gamma = a/g$ where a is the acceleration of the plate and g is gravitational acceleration) of $1.7 \leq \Gamma \leq 1.85$, and a shaking frequency f of $10 \leq f \leq 25$ Hz.

As mentioned in chapter 2 our experiment was originally performed with a shaking frequency of 60 Hz, but the formation of spirals were still found to be fairly common even though this was well outside of the expected region where this should occur. This caused us to look for a frequency region where these spirals did not occur, but this was not found.



Figure 3.8: Example of a tight spiral forming from the blue chain.

It should be noted we did not perform a comprehensive study concerning which frequency spirals will form at, as our shaker set up had only a few frequencies that did not cause some very loud resonance with the apparatus. We eventually settled on a shaking frequency of 20 Hz, with a dimensionless acceleration of $\Gamma = 2.35$, as a good operating range even though spirals still formed. These spirals presented a problem because while spiral formation often resulted in chain separation, we felt that these separations were not the entropic type of separations we were interested in, but rather like the spirals acting as a ratchet pulling the chain into itself (possibly away from the other chain). It was therefore important to find a method to separate pictures that included spirals from those that did not. This also allowed us to briefly look at others factors, such as chain confinement, that may affect spiral formation by looking at which conditions resulted in the highest fraction of pictures with spirals vs ones without.

Like all the other forms of analysis, determining if there was a spiral in a particular picture needed to be automated due to the large number of pictures to be analyzed. The overall idea was that spirals would have a much higher bead density than other arrangements of the chain, so determining some threshold chain density should allow us to sort the pictures. This was complicated by the fact that a small part of a long chain may form a small spiral while the rest of the chain remained unspiraed, which we would not want to include in the 'spiral' category. We were therefore looking for a specific fraction of the total

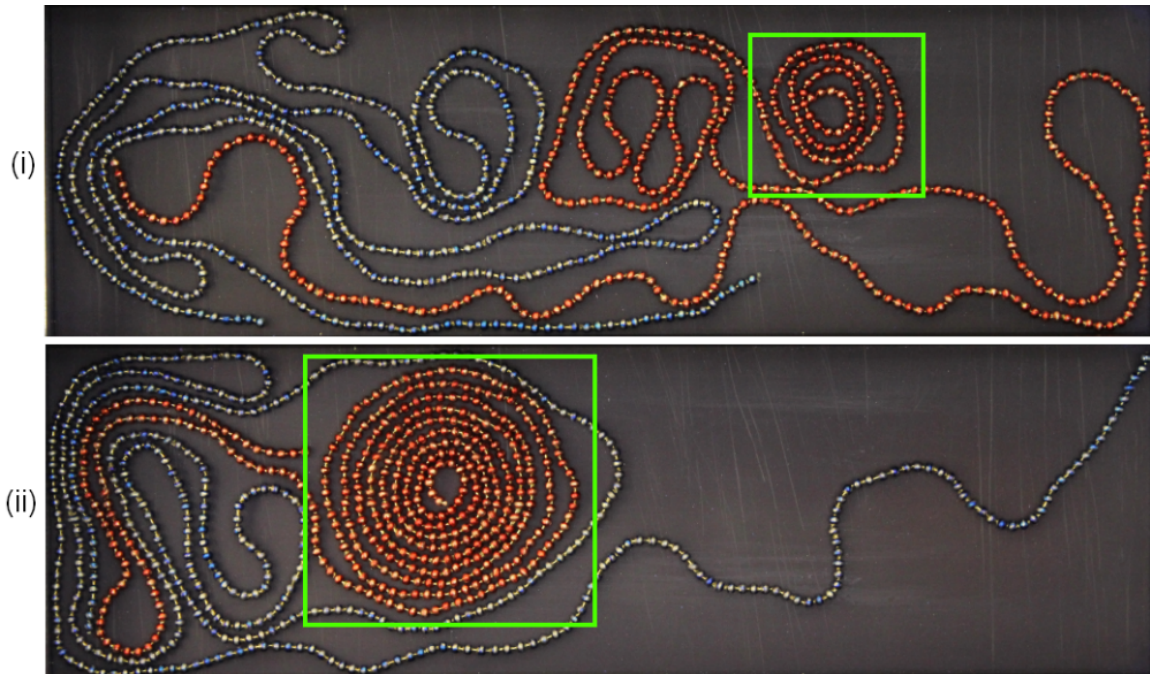


Figure 3.9: Classifying spiral pictures. (i) Though a spiral has formed in the highlighted region the vast majority of the chain is in a non-spiraled state, thus the picture is classified as containing no spirals. (ii) A large fraction of the red chain is part of a spiral in the highlighted region, so the picture is thus considered to contain a spiral.

bead count of the chain packed into some specific density. An example of problem this is shown in Figure 3.9.

Each picture was formed into a two dimensional grid and the amount of beads in each bin were counted (like the 2-D binning method). If greater than a specific fraction of the chains beads (for example 30%) are located in any one bin the chain is counted as being in a spiral. If either chain is in a spiral formation the picture is counted in the spiral category. Another difficulty was choosing a grid size that would be useful for all the conditions we were studying. Too small of a bin and we would not be able to reach the desired fraction of beads for long chains in the bin. Too large and small chains could be entirely packed in a single bin even if they are not spiraled. It was decided that instead of keeping the size of the bins constant across all the different slot sizes and changing the number of bins present, we would keep the number of bins constant and let the size of the bins grow as the slot did. This was acceptable as slot size was proportional to the length of the chain used, so wide slots would have large bins that worked for long chains, and likewise for small slots.

Chapter 4

Results and Discussion

In this chapter, we will discuss results gained from analyzing each experimental run using the methods described in chapter 3. The two main factors we were interested in measuring were how confinement and symmetry affect chain separation. To study how confinement affects separation we kept the slot size constant at 7.6cm X 25.4cm while changing the length of the chain. Table 4.1 displays pertinent information about the lengths of chain used.

Chain Length (cm)	N	R_g (cm)	R_g/D
76	232	6.43	0.846
96	292	7.12	0.937
140	428	8.35	1.099
176	538	9.16	1.205
209	638	9.81	1.291
256	782	10.62	1.397

Table 4.1: Information on the chains used to measure the effects of confinement in a fixed slot size 7.6cm X 25.4cm (ie $D = 7.6cm$)

To measure how symmetry affects separation we intended to keep the level of confinement constant as we changed the size of the slot. For example if we had a measurement for a chain with $R_g = 7.46cm$ and slot width of $D = 5.8cm$ (giving $R_g/D = 1.29$), we could increase the chain length to achieve a $R_g = 9.81cm$ while increasing the slot size to $D = 7.6cm$ ($R_g/D = 1.29$). This keeps confinement constant while changing the symmetry factor $\alpha = D/S_L$ (where S_L is the length of the slot, 25.4 cm).

The experimental runs performed to gather the data for this analysis were done using incorrect assumptions of the R_g values for the chains used. Due to the incorrect R_g assumptions we used chains that we thought would give us constant R_g/D , but in fact the R_g of the chains we used for the more symmetric slot geometries (longer chains) were significantly less than we thought. This led to a decrease in R_g/D as we increased $\alpha = D/S_L$. We attempted to measure the effect of symmetry under two cases, one where R_g/D was relatively low and the other when it was relatively high. Information for these two cases can be viewed in Table 4.2 and 4.3 respectively.

Chain Length (cm)	N	R_g (cm)	D (cm)	R_g/D	α
107	327	7.46	5.8	1.29	0.228
140	428	8.35	7.6	1.10	0.299
209	638	9.81	11	0.89	0.433
287	876	11.1	15.6	0.71	0.614
467	1426	13.34	25.4	0.53	1

Table 4.2: Information on the chains used to measure the effects of symmetry with relatively low confinement. Note R_g/D was intended to be held constant as α was increased.

Chain Length (cm)	N	R_g (cm)	D (cm)	R_g/D	α
160	489	8.82	5.8	1.52	0.228
209	638	9.81	7.6	1.29	0.299
306	934	11.38	11	1.03	0.433
434	1325	12.98	15.6	0.83	0.614
709	2164	15.53	25.4	0.61	1

Table 4.3: Information on the chains used to measure the effects of symmetry with relatively high confinement.

4.1 Spirals

As mentioned in chapter 3, the formation of tight spirals was an unexpected occurrence, and it was unclear how these spirals would effect our results. To check under what conditions spirals occurred most frequently we used the method described in section 3.3 to sort the pictures in spiraled/non-spiraled categories. We then measured what fraction of all the pictures taken for a specific configuration contained spirals, the results of which are displayed in Figures 4.1 and 4.2.

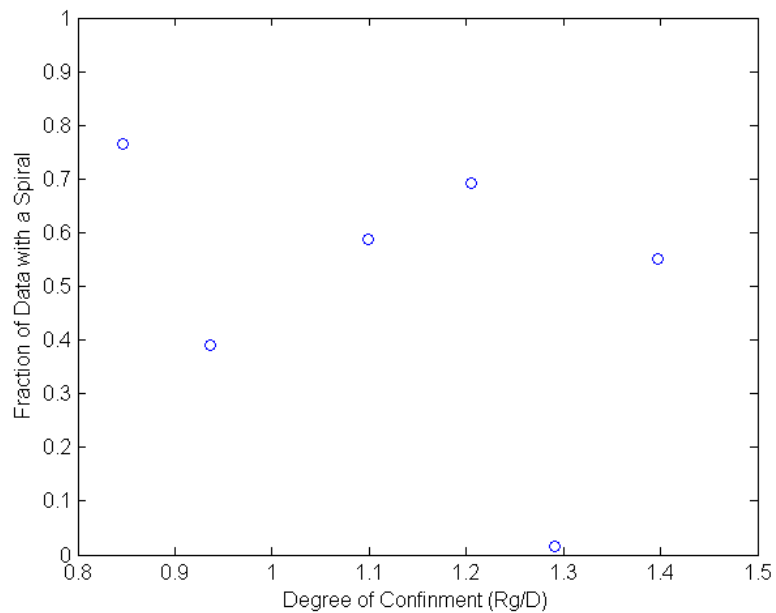


Figure 4.1: The fraction of time each configuration spent with at least one chain in a spiral conformation measured as a function of confinement (slot width fixed at 7.6cm).

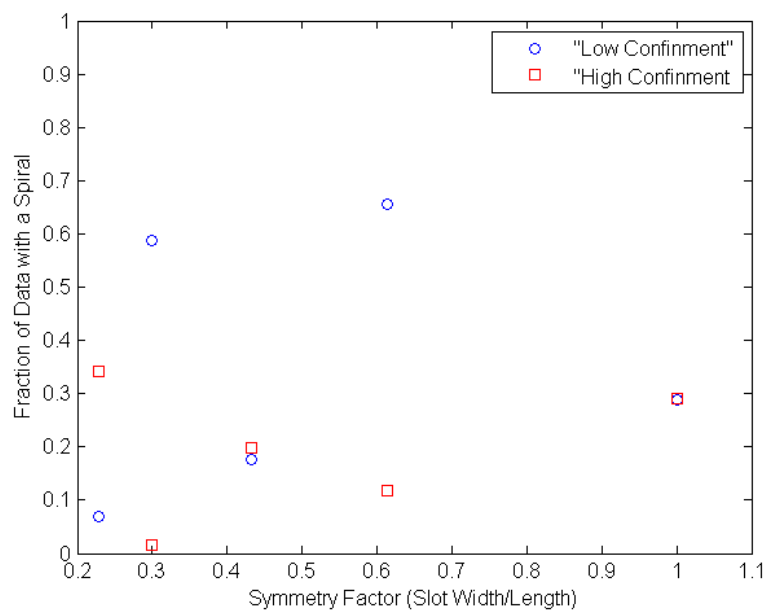


Figure 4.2: The fraction of time each configuration spent with at least one chain in a spiral conformation measured as a function of container symmetry.

As can be seen, there does not appear to be any discernible trend regarding spiral formation either as a function of chain confinement or container symmetry. We observe

that the fraction of data taken that contains spirals can range from nearly all to virtually none. It should be noted that once a spiral forms it generally stays in that conformation for a long period of time, if not the entire length of the run as shown in Figure 4.3. This may be the reason for the high ($\sim 75\%$) percentage of spirals occupying in the least confined state in Figure 4.1, as opposed to the near zero fraction of spirals occurring at $R_g = 1.29$. It may be that the runs at low confinement just happened to enter the spiral state earlier in their runs and stayed that way, while the high confinement case just happened to not enter the state until late in the runs performed. The main issue here, which shall be discussed more in depth in the discussion section of this chapter, is the relative lack of data. While each data point on these plots is formed from the measurement of between 800 to 1200 pictures taken 25 seconds apart (that is to say measuring between 6 and 8 hours of shaking per slot and chain configuration), these points were all gathered from only 4 to 6 long runs. This means that if a run enters the spirals state early it causes close to a quarter of all the data measured for that configuration to be in the spiral state, which may not be an accurate representation of the net behavior that would be observed if hundreds or thousands of runs were performed.

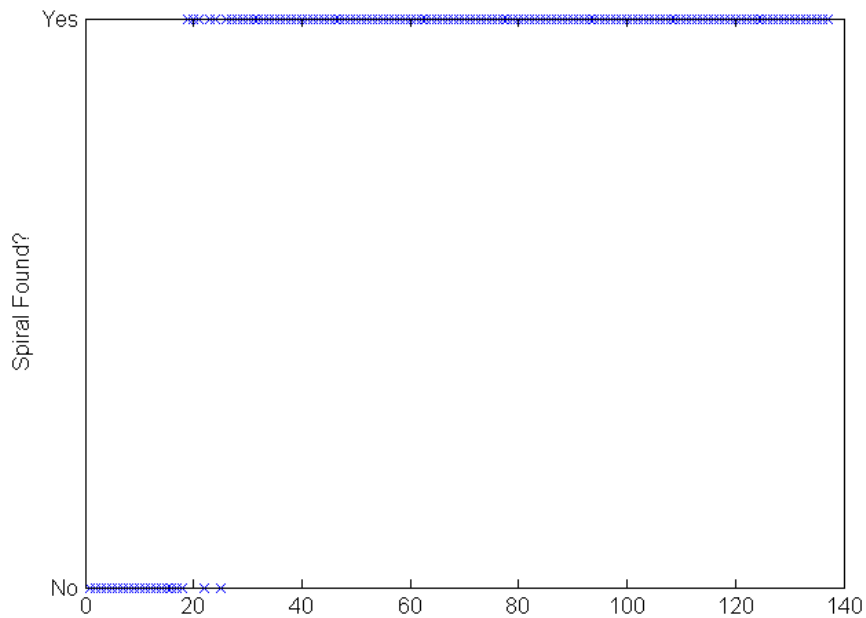


Figure 4.3: Time series showing chain entering and remaining in the spiral state.

4.2 Effects of Confinement

4.2.1 Overlap Method

Figures 4.4 and 4.5 show the effect chain confinement has on chain separation measured using the overlap method. Figure 4.4 shows the average values of the entirety of the data taken while 4.5 shows the averages derived only from the data where no spirals occurred. Two important things can be gathered from these plots. The first is that there does not seem to be any discernible trend of chain separation as a function of confinement. We observe that, using this method, a large amount of the data points are measured as completely mixed with a small amount of completely unmixed that lowers the average from unity (with a very small number of transient states between these two extremes), an example of which is provided in Figure 4.6. The primary reason for this result is that it is very common for one chain to completely run along the slot boundaries and thus encircle the other chain which is measured as completely mixed even if it is only a relatively small amount of the overall chain that is doing the encircling, as shown in Figure 4.7. It should also be noted that the most highly confined case ($R_g = 1.4$) is close to always being mixed (degree of mixing = 99.5%). This is due to the chain being extremely confined and not having sufficient room to maneuver around the container to properly explore all possible configurations, so it would get ‘stuck’ in mixed configurations for the entirety of the run.

The second thing to note is the rather weak effect removing the pictures that contained spirals from the pool of data for a particular configuration. In fact, on average the complete data sets and their spiral-removed counterparts only differ from each other by $\sim 5\%$. This will be a common result for the rest of the results presented in this chapter. The average degree of mixing is 0.90 ± 0.06 .

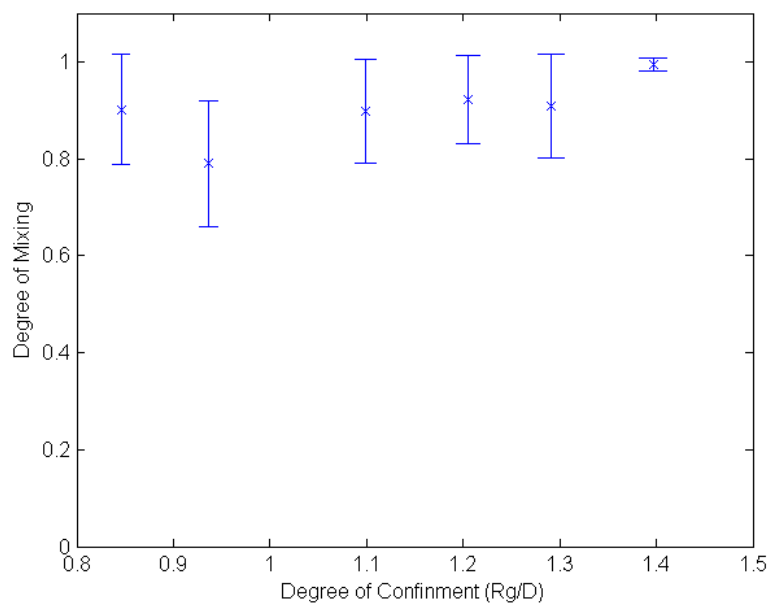


Figure 4.4: Degree of separation as a function of confinement, determined by measuring the size of the overlapping region of the two chains as a fraction of the total region occupied by the more compact chain.

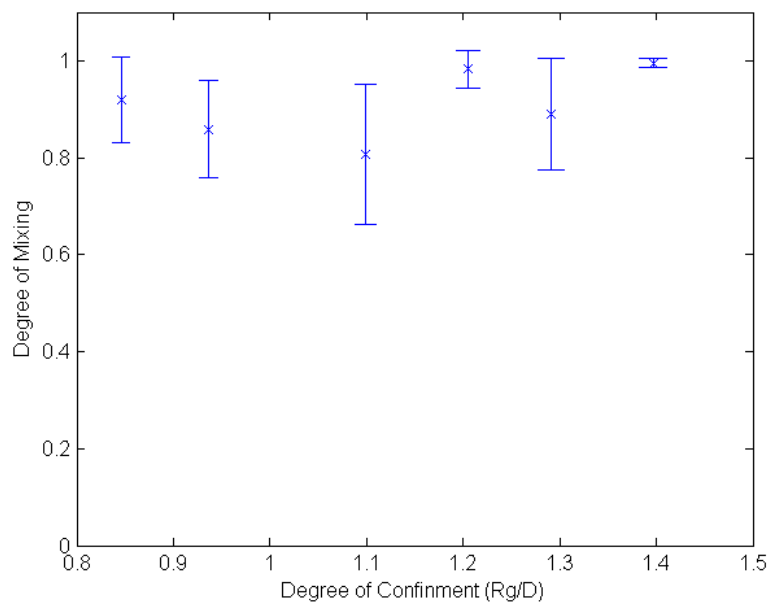


Figure 4.5: Degree of separation as a function of confinement measured with the overlap method. Any picture with a spiral has been filtered out of this data pool.

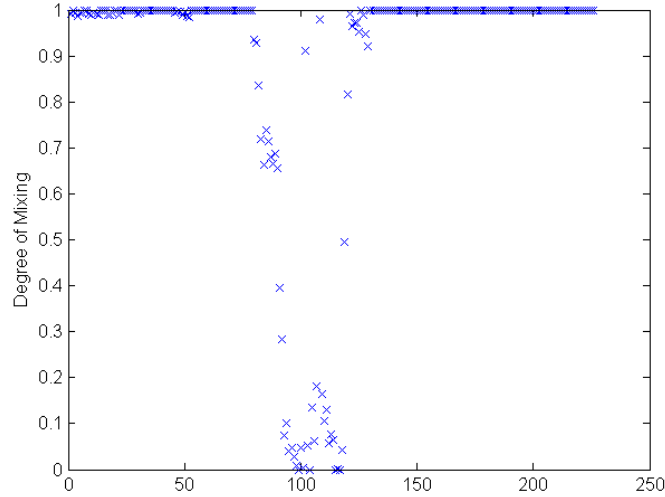


Figure 4.6: Typical time series of separation using overlap method.

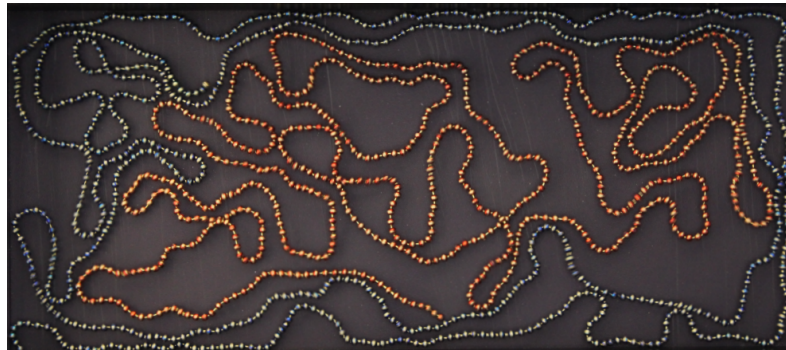


Figure 4.7: An example of how one chain can completely encircle the other.

4.2.2 2-Dimensional Binning

As seen in figures 4.8 and 4.9 the least confined case ($L = 76\text{cm}$, $R_g = 0.846$) is very strongly mixed, especially compared to the rest of the data. This is due to the fact that, in this case, the two chains became and stayed tightly wrapped around one another in a relatively small portion of the container as seen in Figure 4.10. A typical time series of the two dimensional binning method is also shown in Figure 4.11. To better view which trend, if any, the bulk of the data followed an inset was created in these plots that is a zoomed in view of data excluding the least confined outlier. It is apparent that no significant trend is observed using two dimensional binning to measure separation as a measure of confinement, with or without the data that contains spirals is included. The difference between the measurements with

and without the spirals included is significantly more pronounced when using this method, at $\sim 16\%$, with an average degree of mixing (excluding the least confined case) is relatively low at 0.366 ± 0.071 .

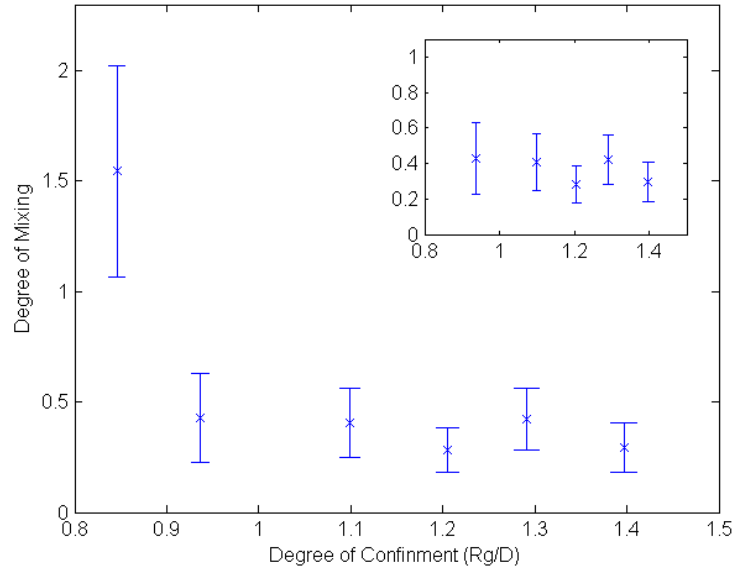


Figure 4.8: Degree of separation as a function of confinement, measured by dividing the slot into 2 dimensional bins. Inset: zoomed view of data excluding the least confined outlier.

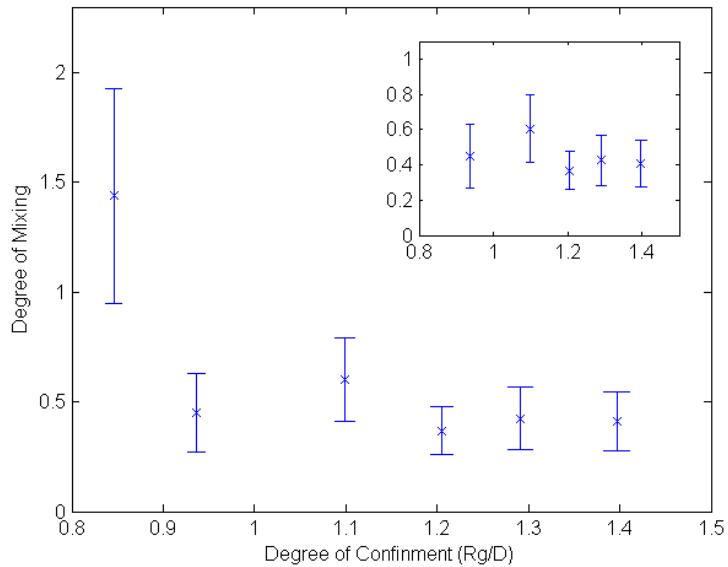


Figure 4.9: Degree of separation as a function of confinement, measured by dividing the slot into 2 dimensional bins with the spirals filtered out. Inset: zoomed view of data excluding the least confined outlier.



Figure 4.10: An example of the type of conformation that caused the strong outlier in Figures 4.7 and 4.8.

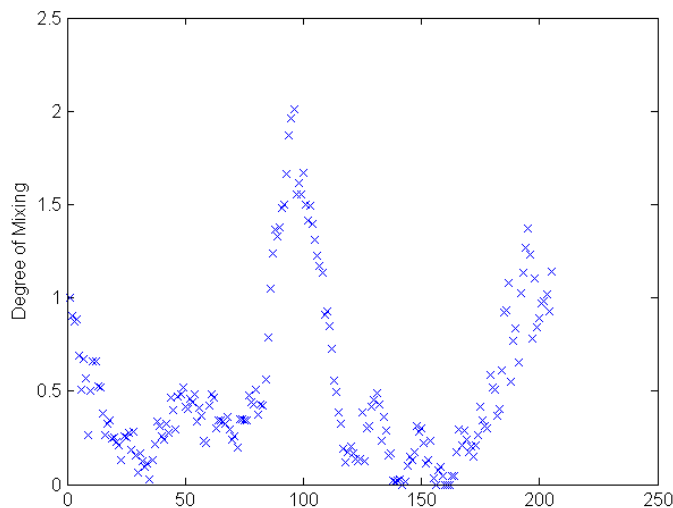


Figure 4.11: Typical time series of mixing using 2D binning.

4.2.3 1-Dimensional Binning

Very similarly to the two dimensional analysis, determining the level of separation using a one dimensional binning method is complicated by the least confined case. Once again, no clear trend with regards to separation as a function of confinement is found when observing the bulk of the data. The average difference between the spiraled and non-spiraled data is relatively small at around 9%, while the average measure of the degree of mixing is 0.686 ± 0.078 . A typical time series of the two dimensional binning method is also shown in Figure 4.14.

Observing the lack of clear trends in either of the above three methods, it would appear that there is no clear correlation between chain confinement and the degree to which these chains will separate, at least within the scope of our data. It should be noted that we have

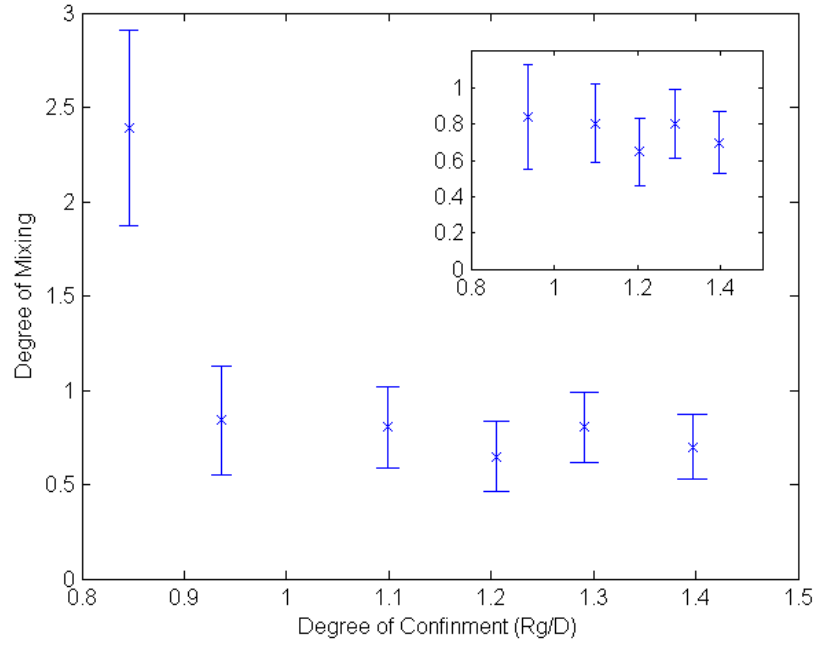


Figure 4.12: Degree of separation as a function of confinement, measured by dividing the slot into 1 dimensional bins. Inset: zoomed view of data excluding the least confined outlier.

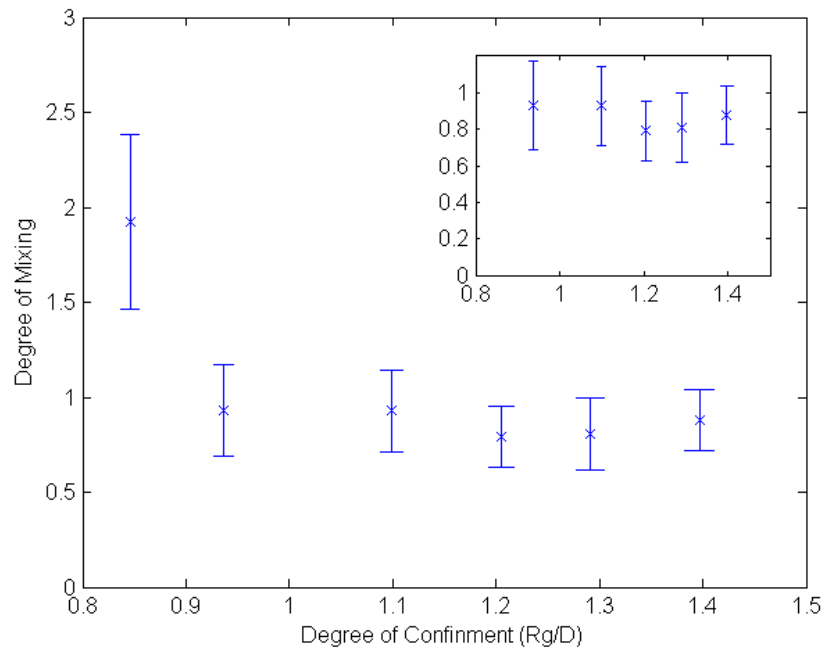


Figure 4.13: Degree of separation as a function of confinement, measured by dividing the slot into 1 dimensional bins with the spirals filtered out. Inset: zoomed view of data excluding the least confined outlier.

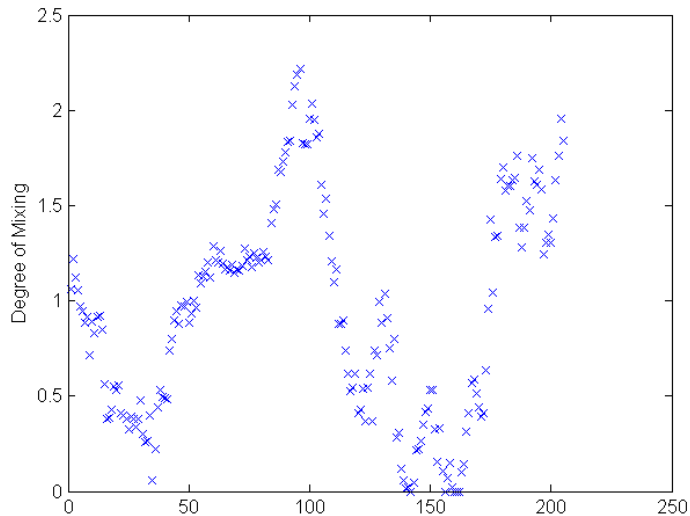


Figure 4.14: Typical time series of mixing using 1D binning.

covered a rather narrow range of confinements in this experiment, but it would be difficult to achieve levels of confinement greater than $R_g/D = 1.4$ with a similar 2-D apparatus.

4.3 Effects of Container Symmetry

As mentioned above, the original intention of measuring the effect of container symmetry on chain separation was to keep the level of confinement (R_g/D) constant as we varied the level of container symmetry ($\alpha = D/S_L$). Unfortunately this was not accomplished as our R_g calculations were incorrect at the time for the chain lengths being used. Instead of staying constant while α was increased R_g instead dropped by $\sim 40\%$ from the most asymmetric ($\alpha = 0.228$) to the most symmetric ($\alpha = 1$) case. Figure 4.15 displayed the phase space that was investigated during this phase of the experiment. Recall that both increasing α and decreasing R_g should decrease the unmixing that occurs according to theory and past simulations. Thus, if we were to see any trends that follow this expectation they should in fact be reinforced by the change in R_g .

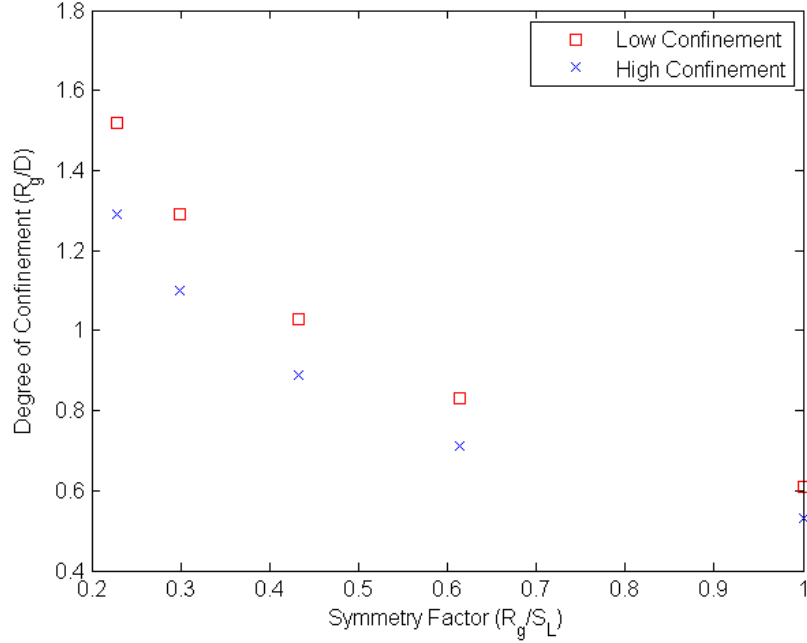


Figure 4.15: Phase space of symmetry and confinement explored.

4.3.1 Overlap Method

Figures 4.16 and 4.17 display the results of using the overlap method to determine the degree of separation as a function of container symmetry with all the data and with the spiral data filtered out respectively. These plots show both the ‘low’ and ‘high’ confinement cases for each container geometry (keeping in mind that the level of confinement is not consistent as geometry changes). There appears to be no discoverable pattern in this data, which has an average level of mixing of 0.884 ± 0.097 . The difference between the entire data pool and the spiral-removed pool is again low at $\sim 4\%$.

4.3.2 2-Dimensional Binning

Similarly Figures 4.20 and 4.21 display this same data using the two dimensional binning method of measuring the separation. Again no visible trend is observed. The mean degree of separation is 0.284 ± 0.125 , with a relatively high difference between the spiral and non-spiral cases of $\sim 12\%$ (with some configurations reaching as high as $\sim 30\%$).

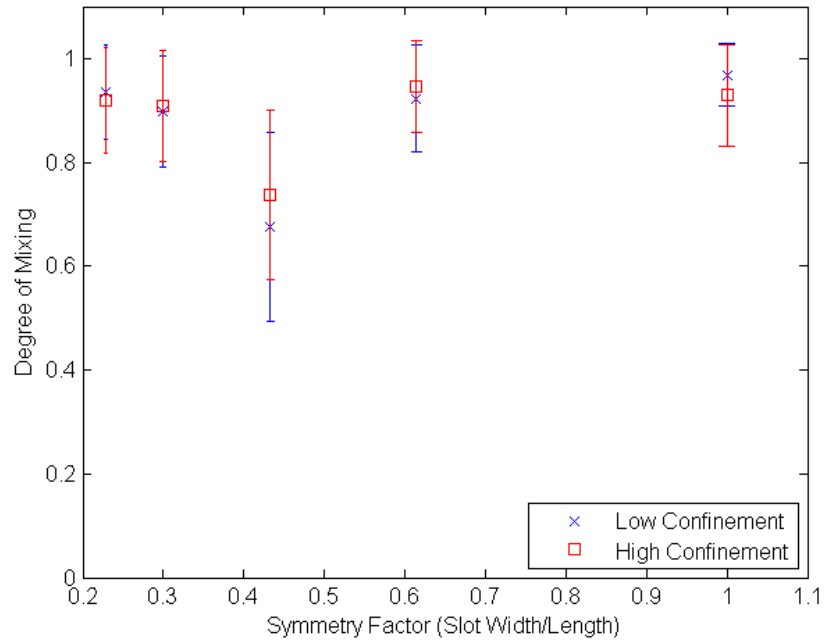


Figure 4.16: Degree of separation as a function of container symmetry, determined by measuring the size of the overlapping region of the two chains as a fraction of the total region occupied by the more compact chain.

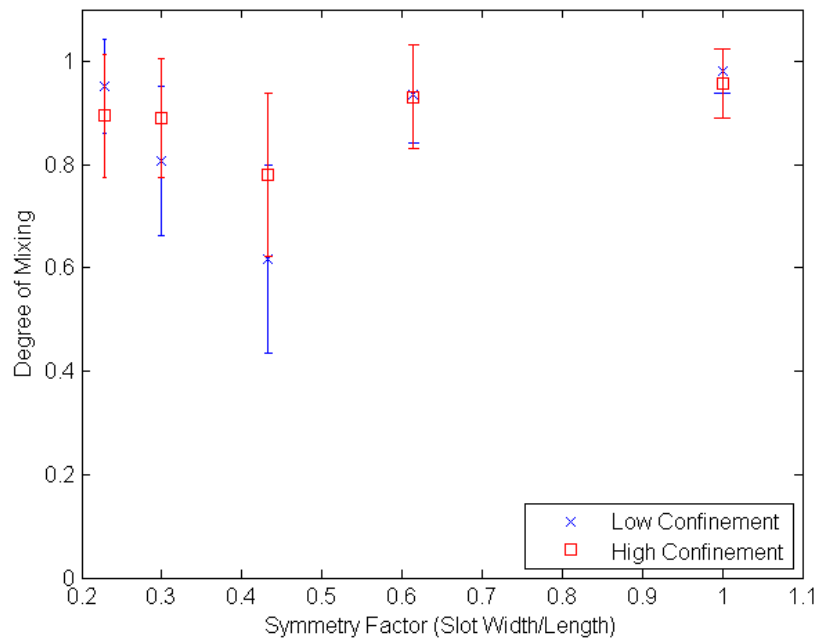


Figure 4.17: Degree of separation as a function of container symmetry measured with the overlap method. Any picture with a spiral has been filtered out of this data pool.

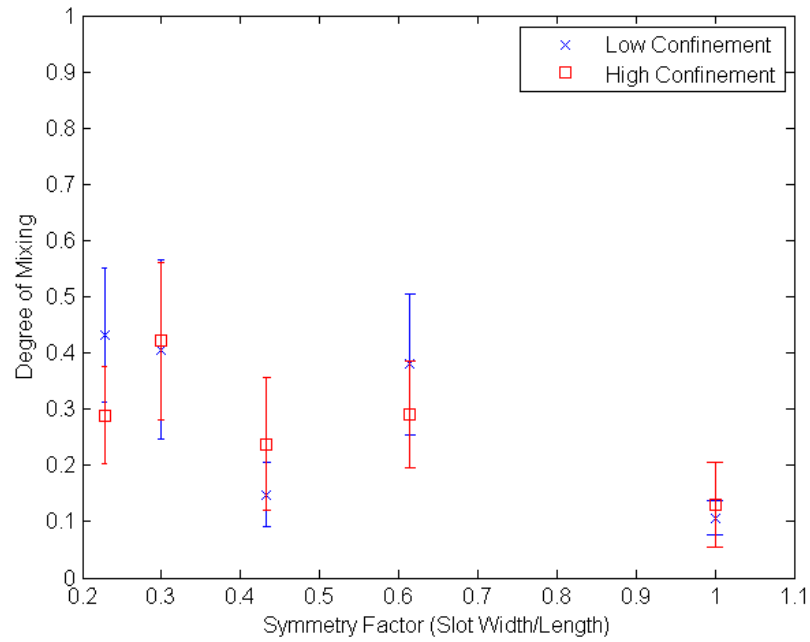


Figure 4.18: Degree of separation as a function of container symmetry, measured by dividing the slot into 2 dimensional bins.

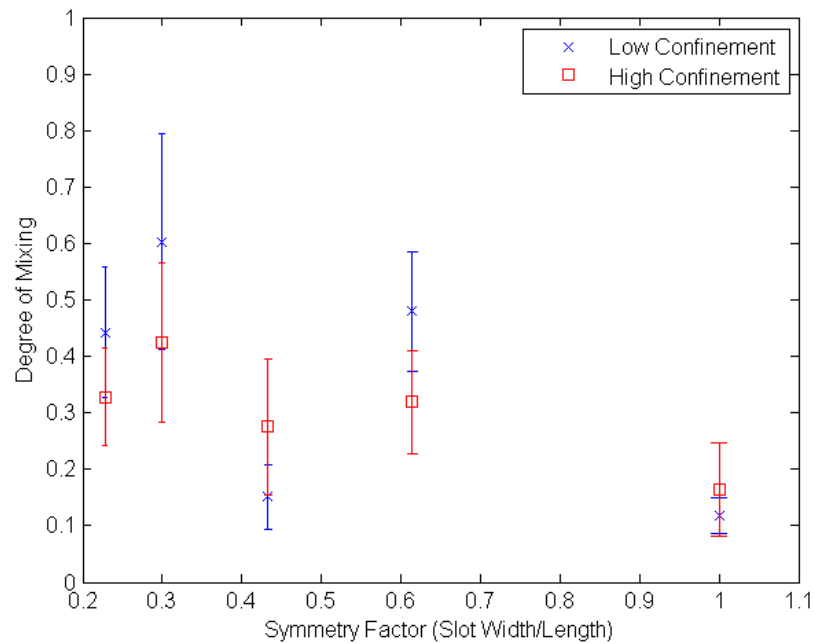


Figure 4.19: Degree of separation as a function of container symmetry, measured by dividing the slot into 2 dimensional bins with the spirals filtered out.

4.3.3 1-Dimensional Binning

The last case we will look at is using one dimensional binning to measure the degree of separation as a function of container symmetry. As with all other cases, no clear trend is observed for either the high or low confinement cases. The average degree of mixing is 0.727 ± 0.116 , with a low difference between the spiral and non spiral data of $\sim 6\%$.

4.4 Discussion

As we have seen, we have not observed any clear relationship between separation and confinement or container geometry, but there are a few problems with our experimental approach that I believe may have caused this. The first and foremost is the relative lack of data. As mentioned before, each data point is made from an average of the analysis of 800 to 1200 pictures (or 6 to 8 hours of shaking). At first glance this may seem like a large amount of data from which to derive a statistical average, but there are so many possible configurations the chains could take that 1000 samples is not nearly sufficient. Previous computer simulations performed to investigate this phenomena have taken many more samples to calculate their statistics, for example Jacobsen [13] took at least 30,000 samples for each configuration investigated. It is unclear if we would still observe the same lack of trends if we were able take a similar number of samples per configuration, but this would be difficult and time consuming to do experimentally.

Another barrier that may have prevented us from observing the chain separation that was expected was the geometry and design of the shaking system. As mentioned above, the formation of spirals in the chains was a significant source of frustration. We did not expect them to be formed and we felt that even if the spirals occurred during separation, it was possible it was the spirals ratcheting behavior that drove the separation instead of the entropic effects we wished to study. We were very surprised that sampling only the pictures that did not include spirals did not drastically change the measurements of separation. It seems there are a roughly equal number of spirals that form at all degrees of mixing, which is to say there are as many spirals that result in complete separation and complete mixing (as well as all states in between).

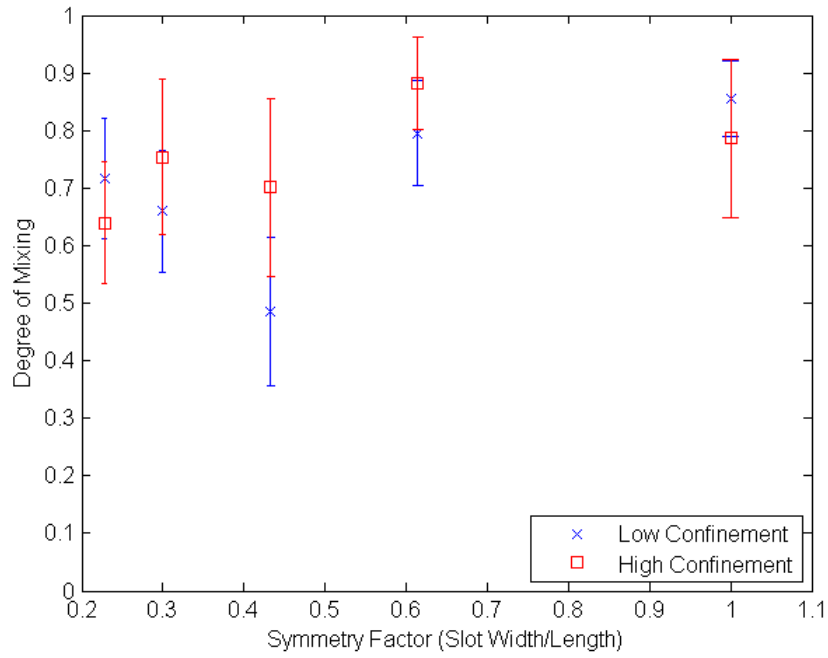


Figure 4.20: Degree of separation as a function of container symmetry, measured by dividing the slot into 1 dimensional bins.

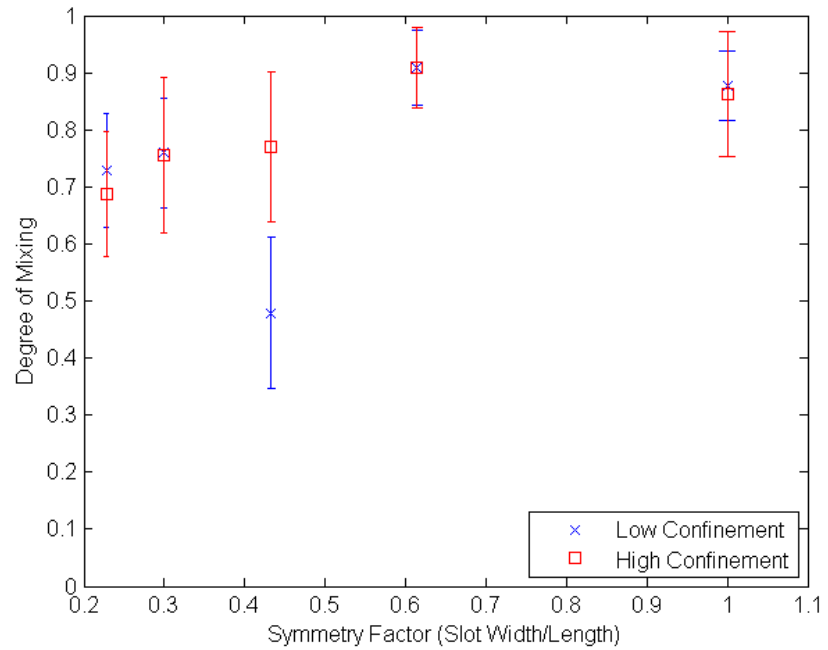


Figure 4.21: Degree of separation as a function of container symmetry, measured by dividing the slot into 1 dimensional bins with the spirals filtered out.

4.4.1 Future Work

The main barrier to taking a more appropriate number of samples is that each run of 200 or so samples requires around a day of preparation to colour and varnish each chain. If instead of differentiating the chains through colour it was possible to track the chains by following their links then it would be simple to cut two lengths of chain and use them immediately (and indefinitely as there is no colour to wear off). This would save a great deal of time and effort, and though it was unsuccessfully attempted during this project it may be worthwhile to investigate in the future.

Preventing spirals from forming should be a priority for any similar future projects. If they intend to use a similar 2D slot apparatus it may be beneficial to attach smaller beads to the surface of the plate and walls, which was successful in preventing spiral formation in [14] by Safford. It may also be possible to find a shaking frequency that does not produce spirals, though none were found in this project.

In an ideal world, this experiment would be performed in a long cylindrical tube (ie in three dimensions) rather than the 2D analog of the slot. This would obviously be much more complicated to accomplish experimentally but would be a closer analog to bacterial cells, as well as completely eliminating the spiral problem.

4.5 Conclusion

While no appreciable insights into the validity of the theories of entropically driven polymer separation were gained, valuable developments on the shaking system were implemented that may be used in future shaking experiments. Though we did not observe any trends that would support past theories and simulations on this matter, we can also not use any of these results to weaken these theories either, primarily due to the insufficient amount of data collected and analyzed. It is my hope that the work done on the shaker system, and possibly the data regarding chain separation we obtained, be of use in future graduate research.

Bibliography

- [1] S.L. Kline-Smith and C.E. Walczak, Mitotic spindle assembly and chromosome segregation: refocusing on microtubule dynamics. *Mol. Cell* **15** (2004), pp. 317-327
- [2] F. Jacob and S. Brenner, On the regulation of DNA synthesis in bacteria: the hypothesis of the replicon. *C. R. Hebd. Seances. Acad. Sci* **256** (1963), pp. 298-300
- [3] K.P. Lemon and A.D. Grossman,, The extrusion-capture model for chromosome partitioning in bacteria. *Genes Dev.* **15** (2001), pp. 2031-2041
- [4] J. Dworkin and R. Losick, Does RNA polymerase help drive chromosome segregation in bacteria? *Proc. Natl. Acad. Sci. U.S.A.* **99** (2004), pp. 14089-14094
- [5] C.D. Webb et al, Use of time-lapse microscopy to visualize rapid movement of the replication origin region of the chromosome during the cell cycle in *Bacillus subtilis*. *Mol. Microbiol* **28** (1998), pp. 883-892
- [6] R.B. Jensen, S.C. Wang and L. Shapiro, A moving DNA replication factory in *Caulobacter crescentus*. *EMBO J* **20** (2001), pp. 4952-4963
- [7] P.J. Lewis, S.D. Thaker and J. Errington, Compartmentalization of transcription and translation in *Bacillus subtilis*. *EMBO J.* **19** (2000), pp. 710-718
- [8] S. Jun and B. Mulder, Entropy-driven spatial organization of highly confined polymers: lessons for the bacterial chromosome. *Proc. Natl. Acad. Sci. U.S.A.* **103** (2006), pp. 12388-12393.
- [9] S. Jun and A. Wright,, Entropy as the driver of chromosome segregation. *Nat. Rev. Microbiol.* **8** (2010), pp. 600-607.

- [10] P.J. Flory and W.R. Krigbaum, Statistical Mechanics of Dilute Polymer Solutions. II. *J. Chem. Phys.* **18** (1950), pp. 1086-1094.
- [11] A.Y. Grosberg, P.G. Khalatur, and A.R. Khokhlov, Polymeric coils with excluded volume in dilute solution: the invalidity of the model of impenetrable spheres and the influence of excluded volume on the rates of diffusion-controlled intermacromolecular reactions *Die Makromol Chem. Rapid Commun.* **3** (1982), pp. 709-713.
- [12] M. Benmouna et al, Scattering Properties and Phase Behavior of Mixtures of Cyclic and Linear Homopolymers and Copolymers *Macromolecules* **30** (1997), pp. 1168-1172.
- [13] J. Jacobsen, Demixing of compact polymer chains in three dimensions *Phys. Rev E.* **82** (1997), 051802.
- [14] K. Safford et al, Structure and dynamics of vibrated granular chains : Comparison to equilibrium polymers *Phys. Rev E.* **79** (2009), 061304.
- [15] Y. Jung et al, Ring polymers as model bacterial chromosomes: confinement, chain topology, single chain statistics, and how they interact *Soft Matter* **8** (2012), pp. 2095-2102.
- [16] R.E. Ecke, Spontaneous spirals in vibrated granular chains *MRS Symposia Proceedings* **759** (2012), pp. 129-133.